Chemical Engineering Journal 150 (2009) 181–187

Contents lists available at ScienceDirect

Chemical Engineering Journal

journal homepage: www.elsevier.com/locate/cej

Separation of binary heavy metals from aqueous solutions by nanofiltration and characterization of the membrane using Spiegler–Kedem model

Z.V.P. Murthy*, Latesh B. Chaudhari

Department of Chemical Engineering, S.V. National Institute of Technology, Ichhanath, Surat 395007, Gujarat, India

ARTICLE INFO

Article history:
Received 16 June 2007
Received in revised form 15 December 2008
Accepted 16 December 2008

Keywords:
Nanofiltration
Concentration polarization
Membrane transport model
Membrane characterization

ABSTRACT

Heavy metals are important sources of environmental pollution and are non-degradable, and therefore, continue to exist in water. Membrane technology is one option for the separation of heavy metals from wastewater without generating any pollution load. This paper presents the binary heavy metals (cadmium and nickel) separation capability of a commercial nanofiltration membrane from aqueous solutions. The influence of applied pressure, feed solute concentration, feed flowrate, feed pH and nature of anion on the retention of cadmium and nickel ions is studied. It is observed that the rejection increases with increase in feed pressure and decreases with increase in feed concentration at constant feed flowrate. The maximum observed solute rejection of nickel and cadmium ions are 98.94% and 82.69%, respectively, for an initial feed concentration of 5 ppm. The NF membrane is characterized by using the Spiegler–Kedem model based on irreversible thermodynamics coupled with film theory. Boundary layer thicknesses, as well as the membrane transport parameters are estimated by using the Levenberg–Marquardt method. The estimated parameters are used to predict the membrane performance and found that the predicted values are in good agreement with the experimental results.

1. Introduction

Heavy metals are extremely toxic and have a tendency to bioaccumulate in the food chain. The only way to remove them is to change their chemical and physical states by oxidation/reduction and precipitation. So far, there have been a number of researches that studied physical and chemical treatments of heavy metals from wastewater [1–5]. However, these methods may not be cost effective and contribute to other problems such as slag disposal and extra chemical injection. Membrane technology had also gained its popularity in metal separation/rejection by reverse osmosis (RO) and ultrafiltration (UF) [6,7]. However, problems like high operation and maintenance cost for application of high pressure to the system and pretreatment necessity have led to the production of NF membranes. There are successful studies utilizing NF as tool for removal of heavy metals ions [8–10]. The rejection of solutes by NF membranes is mainly influenced by two basic membrane characteristics; membrane charge and membrane pore size. In the charge exclusion, a Donnan potential is created between the charged anions in the NF membranes and the co-ions in the influent.

Separations on single metal ions from aqueous solutions were reported in the literature, but the same on binary metals is feeble. The present work is aimed in this direction. Separation of heavy metals from binary aqueous solutions ($CdCl_2$–$NiSO_4$–water) using a commercial thin film composite polyamide nanofiltration membrane has been studied. The performance of the NF membrane and its characterization based on an irreversible thermodynamics model (Spiegler–Kedem model) is reported. The concentration polarization boundary layer thicknesses, as well as the membrane transport parameters from permeation data are determined. Experiments with binary aqueous solutions ($CdCl_2$–$NiCl_2$–water) and ($CdSO_4$–$NiSO_4$–water) are performed to know the influence of the anion on the separation of nickel and cadmium ions.

2. Materials and methods

Synthetic samples of wastewater are prepared by adding required amounts of cadmium chloride ($CdCl_2{\cdot}2H_2O$), cadmium sulphate ($CdSO_4{\cdot}8H_2O$), nickel chloride ($NiCl_2{\cdot}6H_2O$) and nickel sulphate ($NiSO_4{\cdot}6H_2O$) to distilled water. Several solutions are prepared with different concentrations of cadmium chloride and nickel sulphate (5–250 ppm). The experiments are performed on a Perma®-pilot scale membrane system (Permionics, Vadodara, India), shown in Fig. 1. A rectangular flat membrane housing cell is used for the experiments. The membrane housing cell, shown in Fig. 1, is made of stainless steel with two halves fastened together

* Corresponding author. Tel.: +91 261 2201641/2223371–2223374; fax: +91 261 2201641/2227334.
E-mail addresses: zvpm2000@yahoo.com, zvpm@ched.svnit.ac.in (Z.V.P. Murthy).

1385-8947/$ – see front matter © 2008 Elsevier B.V. All rights reserved.
doi:10.1016/j.cej.2008.12.023

Nomenclature

C_{Ai}	concentration of A at any position i (kmol/m^3)
D_{AB}	diffusion coefficient of solute A in solvent B
J_V	permeate volume flux (m^3/m^2 s)
L_P	hydraulic permeability (m/s kPa)
ΔP	pressure difference across the membrane (kPa)
P_M	overall solute permeability (m/s)
P_s	local solute permeability in the membrane
R	true solute rejection
R_g	universal gas constant (8.314 J/gmol K)
R_O	observed solute rejection
T	temperature (K)
x	coordinate direction perpendicular to the membrane (m)
Δx	total membrane thickness (m)

Greek letters

δ	boundary layer thickness on high pressure side of the membrane (m)
$\Delta\pi$	osmotic pressure difference across the membrane (kPa)
σ	reflection coefficient
ν	total number of ions dissociated from 1 mol of salt
ϕ	osmotic coefficient based on the solute concentration at the membrane surface
β	$J_V(1-\sigma)/P_M$

Subscripts

A	solute
B	solvent
M	membrane
1	feed solution
2	boundary layer solution
3	permeate solution

with high tensile bolts. The top half of cell contained the flow distribution chamber and the bottom half is used as the membrane support system. The upper half of the test cell contains a groove for the arrangement of HDPE 'O' ring to avoid leakage at high pressure operation. Experiments are performed with a commercial thin film composite polyamide membrane Perma-TFC-NF-300 (Permionics, Vadodara, India), hereafter referred as NF-300 membrane. This membrane has three layers. The first layer is a 5–20 μm polyamide layer that does the actual separation/rejection. The second layer is made of polysulfone substrate of about 50 μm thickness. The third layer, used for resistance and strength, is made of polyester with a thickness of about 200 μm. The Perma-TFC membranes are capable of withstanding pH in the range 2–12, pressure up to 30 atm and temperatures up to 50 °C. In the present work all the experiments are performed at a pH of 5.0. The NF-300 membrane is characterized by 300 Da cut-off. The effective membrane surface area is 150 cm^2 (length 15 cm and width 10 cm). The 2 mm thin channel passage in the membrane test cell and the high cross-flow feed rates used in the experimentation will enable the system in controlling the concentration polarization to some extent. Before conducting the actual experiments, the NF-300 membrane is subjected to stabilization at 20 atm, which is the maximum pressure used in the experiments, for 2 h to avoid possible membrane compaction during the experimentation. Experiments are performed for 2 h, for each set of separation data, in batch circulation mode and the permeate samples are collected from high pressure to low pressure for a particular feed concentration and feed flowrate. Both permeate and concentrate are returned to the feed vessel in order to keep the constant concentration. Samples of permeate are collected at a given time interval, to measure the observed salt rejection, R_O ($=1-C_{A3}/C_{A1}$); where C_{A1} is the bulk feed solute concentration and C_{A3} is the permeate solute concentration; and permeate volume flux (J_V). The metal ion concentrations are measured by an Atomic Absorption Spectrophotometer SL-173 (M/S. ELICO Limited, Hyderabad, India) according to standard methods [11]. After each set of experiments, for a given feed concentration, the setup is rinsed with distilled water for 30 min at 4 atm to clean the system. This procedure is followed by measurement of pure water permeability (PWP) with distilled water to ensure that the initial membrane PWP is restored. The experiments are carried out for different feed concentrations (5, 50, 100, 150, 200 and 250 ppm each of cadmium and nickel salts), feed flowrates (5, 10 and 15 L/min), applied pressures (4, 8, 12, 16 and 20 atm), feed pH (1, 3, 5, 7 and 9) and the corresponding R_O and J_V are measured.

3. Membrane transport parameters and boundary layer thickness

3.1. Combined membrane transport and concentration polarization model

Concentration polarization must be incorporated into an RO/NF/UF model in order to determine the true solute rejection, R ($=1-C_{A3}/C_{A2}$), of the membrane that is based on the solute concentration at the high pressure side of the membrane surface (C_{A2}) in contrast to the observed rejection which is based on the bulk feed concentration. Concentration polarization is typically described via a film theory model whereby it is characterized by the thickness of the boundary layer across which the counter diffusion occurs, as shown schematically in Fig. 2. This boundary layer thickness decreases with increase in the feed flowrate. Hence, some prior studies have attempted to eliminate concentration polarization by using high feed flowrates. However, Yaroshchuk [12] has mentioned that to ignore concentration polarization, the boundary layer thickness must be less than 10 μm, which may not be possible with laboratory-scale experiments. Gupta et al. [13] developed a novel protocol to characterize NF and RO membranes that employ the Spiegler–Kedem membrane transport model coupled with the film theory description of the concentration polarization. Attempts have been made to correct the boundary layer thicknesses determined from literature correlations for the transmembrane flow effects, which are described in the excellent review of Gekas and Halstrom [14].

It can be seen from Fig. 2 that the solute flux through the membrane is given by the product of the permeate volume flux (J_V) and permeate solute concentration (C_{A3}). From simple mass balance, transport of solute at any point within the boundary layer can be described by the relation [15],

$$J_V C_A - D_{AB}\frac{dC_A}{dx} = J_V C_{A3} \tag{1}$$

where x is the coordinate perpendicular to the membrane surface. The mass balance, Eq. (1), can be integrated over the thickness of the boundary layer to give well-known polarization equation [15],

$$\left(\frac{C_{A2}-C_{A3}}{C_{A1}-C_{A3}}\right) = \exp\left(\frac{J_V\delta}{D_{AB}}\right) \tag{2}$$

where δ represents the boundary layer thickness in high pressure side and D_{AB} is the diffusivity of solute A in solvent B.

3.2. Modified irreversible thermodynamics model

An irreversible thermodynamic Spiegler–Kedem model [16] was applied to explain the separation performance of an uncharged

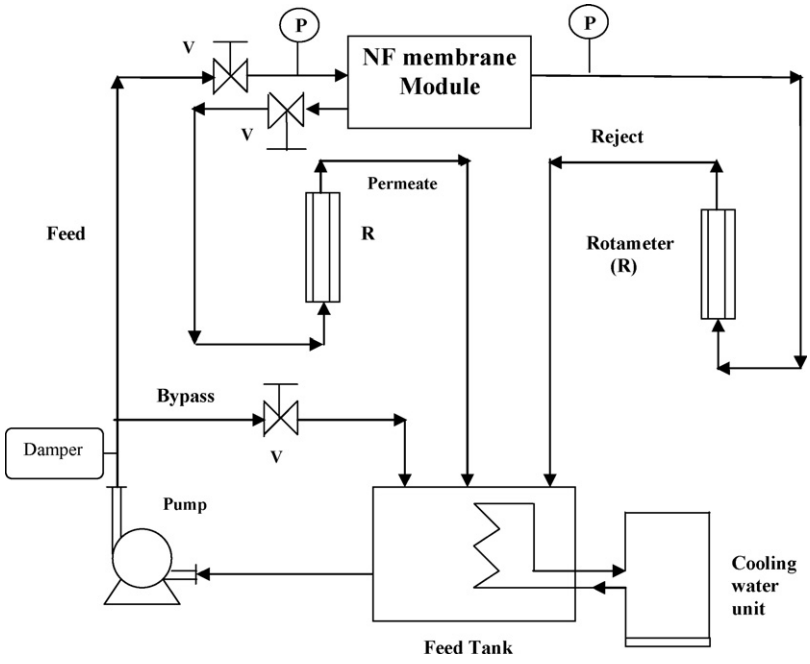

Fig. 1. Perma®-pilot scale membrane system.

solute. Many authors [17–19] have extended this model to explain the retention of electrolyte with an NF membrane that is charged. Spiegler and Kedem [16] applied the linear relationship between fluxes and driving forces on a local level at steady-state and integrated them across the membrane to obtain the following equations:

$$J_V = L_P(\Delta P - \sigma\Delta\pi) \tag{3}$$

$$R = \frac{\sigma[1 - e^{-J_V(1-\sigma)\Delta x/P_s}]}{1 - \sigma e^{-J_V(1-\sigma)\Delta x/P_s}} \tag{4}$$

where P_s is the local solute permeability and $\Delta\pi$ is the osmotic pressure difference across the membrane. Let $P_M = P_s/\Delta x$ and $\beta = J_V(1-\sigma)/P_M$, then Eq. (4) becomes

$$R = \frac{\sigma(e^{\beta} - 1)}{e^{\beta} - \sigma} \tag{5}$$

Here, reflection coefficient (σ) represents the solute separation capability of a membrane, i.e., $\sigma = 0$ means no separation and $\sigma = 1$ means 100% separation, P_M is the overall solute permeability and L_p is the hydraulic permeability of the membrane. The

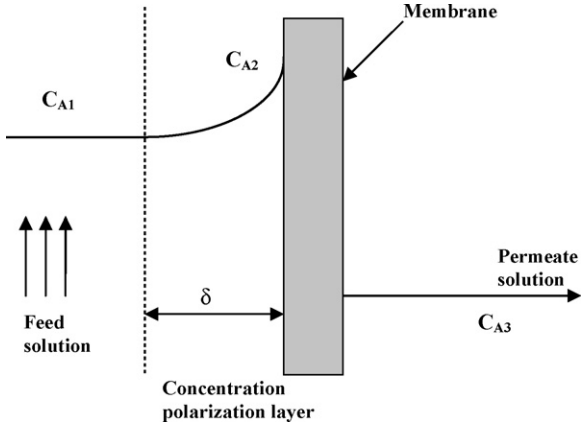

Fig. 2. Schematic of concentration profile on the solute in the feed and permeate solution near the membrane surface.

Spiegler–Kedem model was used widely to interpret/predict the performance of RO/NF/UF membranes [20–24]. The $\Delta\pi$ is given by the van't Hoff equation [13],

$$\Delta\pi = \phi\nu(C_{A2} - C_{A3})R_gT \tag{6}$$

Here, ϕ is the osmotic coefficient for a non-ideal solution that is based on the solute concentration at the membrane surface, ν is the total number of ions dissociated from 1 mol of salt, R_g is the Universal gas constant, and T is temperature. The values of osmotic coefficients of the salts studied here are taken from the literature [25,26]. It is important to note that, due to the concentration polarization, the salt solution at the membrane surface cannot be assumed to be dilute. The values of osmotic coefficients used in this study are 0.534 and 0.584 for cadmium chloride and nickel sulphate salts, respectively. Substituting $\Delta\pi$ from Eq. (6) into Eq. (3), will give:

$$J_V = L_p[\Delta P - \sigma\phi\nu(C_{A2} - C_{A3})R_gT] \tag{7}$$

The J_V and R cannot be directly used to analyze the permeation data since they contain boundary layer concentration (C_{A2}) that cannot be measured directly. Combining Eqs. (7) and (2) will eliminate the term ($C_{A2} - C_{A3}$) and the resulting equation for the permeate flux can be written as [13],

$$J_V = L_p\left[\Delta P - \sigma\phi\nu(C_{A1} - C_{A3})R_gT\ \exp\left(\frac{J_V}{D_{AB}/\delta}\right)\right] \tag{8}$$

By rearranging Eq. (8), one can get

$$\Delta P = \frac{J_V}{L_p} + \sigma\phi\nu(C_{A1} - C_{A3})R_gT\ \exp\left(\frac{J_V}{D_{AB}/\delta}\right) \tag{9}$$

Eq. (9) is the combined membrane transport and concentration polarization model used in the study.

4. Results and discussion

4.1. Influence of operating variables

The R_O is plotted against J_V at different feed solute concentrations (see Fig. 3). It can be seen from Fig. 3 that the R_O increases

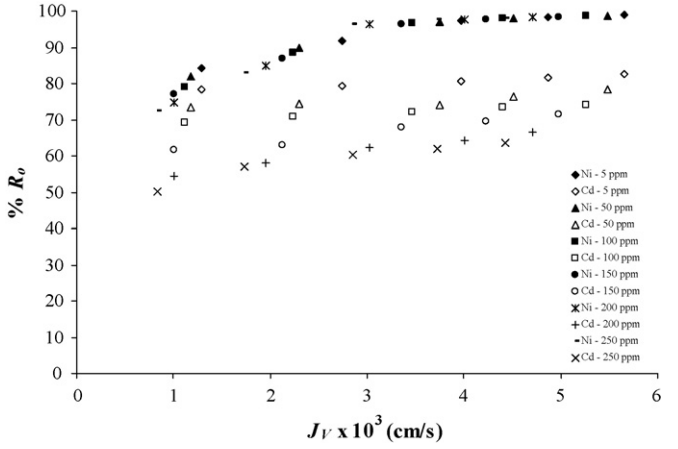

Fig. 3. Relation between permeate volume flux and observed solute rejection for $CdCl_2$–$NiSO_4$–water system of different feed concentrations and feed flowrate 5 L/min.

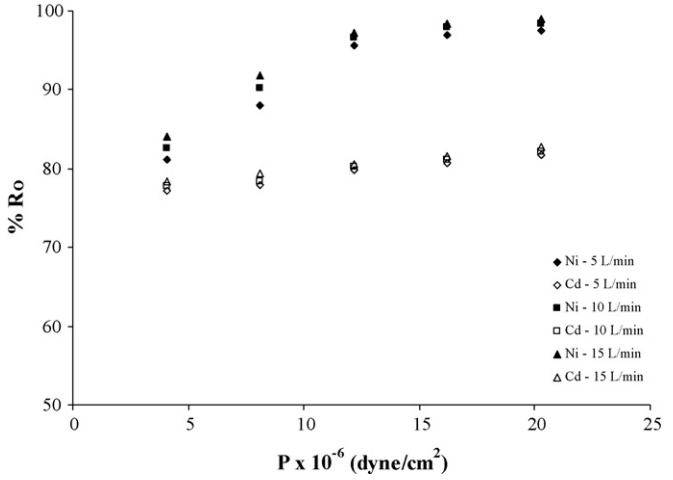

Fig. 5. Influence of applied pressure on the solute rejection of $CdCl_2$–$NiSO_4$–water system at different feed flowrates and feed concentration 5 ppm.

slightly with increase in permeate flux for different feed concentrations from 5 to 250 ppm. Figs. 3 and 4 show the effect of applied pressure on J_V and R_O of binary salts at different concentrations. The rejection increases with increase in feed pressure from 4 to 20 atm. A high diffusive transport of solute through the membrane, compared to convective transport, may be the reason for low retention at low pressure and high feed concentrations [18]. The NF-300 membrane shows the following rejection in sequence: $R_O(Ni^{2+}) > R_O(Cd^{2+})$ for $NiSO_4$–$CdCl_2$–water system, which is typical phenomena of NF membrane [18,27]. The chloride ions are less hydrated than the sulphate ions (1047 and 325 kJ mol/L for chloride and sulphate, respectively) resulting in less rejection of cation associated to chloride ion [17,18,28]. Rejection will increase with higher valency of the anion owing to increased electrostatic repulsion by the membrane [28]. The rejection percentages with change in applied pressure at different feed flowrates in the range of 5–15 L/min, at 5 ppm feed solute concentration are shown in Fig. 5. It can be seen from Fig. 5 that increase in feed flowrate leads to slight increase in the rejection of cadmium and nickel ions. It can also be seen from Fig. 6 that the permeate flux increases with increase in feed flowrate at the same applied pressure. These observations indicate that there is a concentration polarization boundary layer at the surface of the membrane. The main aim of increasing the feed flowrate is to increase the mass transfer coefficient, D_{AB}/δ, which in turn increases the solute rejection. Similar results were found for the nickel ions by Ahn et al. [10] and for the zinc ions by Frares et al. [29]. Although the repulsion of the anion mainly determines the rejection of salt from a solution, it is also interesting to compare the rejection of salts when the same anion is associated with different cations. It can be seen from Figs. 7 and 8 that the rejection of Ni^{2+} is higher than the rejection of Cd^{2+}. An explanation for the experimentally determined rejection sequence can be found by comparing the diffusion coefficients of the different cations. The diffusion coefficient of cations Ni^{2+} and Cd^{2+} in water at 25 °C are 1.32×10^{-5} and 1.44×10^{-5} cm^2/s [30]. It is assumed that the diffusion coefficients in the membrane can be approximated by those in aqueous solutions. The order of diffusion coefficients is inversely reflected in the rejection sequence, so the diffusion seems to be an important transport mechanism. As the diffusion coefficient of Cd^{2+} is higher than that of Ni^{2+}, a high diffusion contribution can be expected resulting in a lower rejection. Similar trends were observed by Mohammad et al. [8]. It can also be seen from Figs. 7 and 8 that the separation of both Cd^{2+} and Ni^{2+} are enhanced when the charge valency of the associated co-ion is increased.

Fig. 9 shows the effect of pH on rejection of nickel and cadmium ions for $CdSO_4$–$NiSO_4$–water and $CdCl_2$–$NiCl_2$–water systems. The pH is adjusted by the addition of HCl and NaOH, depending upon the need. The concentration, pressure and flowrate are

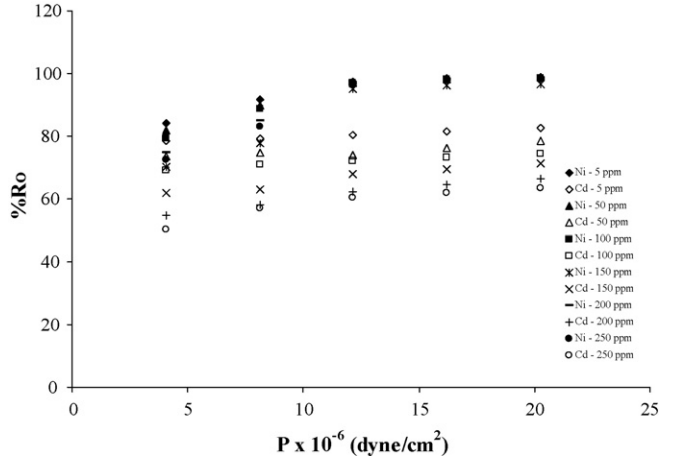

Fig. 4. Influence of applied pressure on the observed solute rejection of $CdCl_2$–$NiSO_4$–water system with different feed concentrations at feed flowrate 5 L/min.

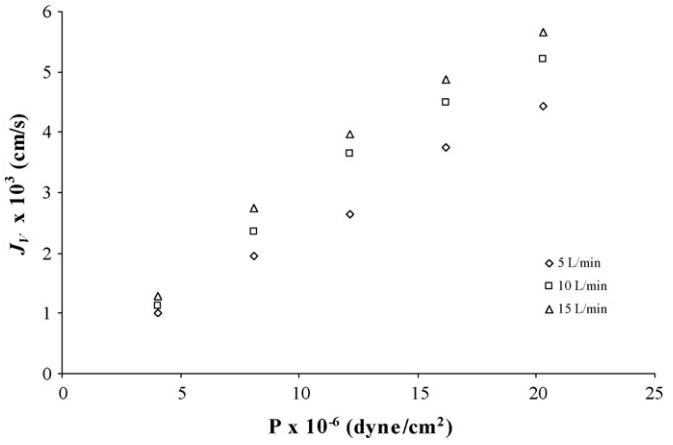

Fig. 6. Influence of applied pressure on the permeate volume flux of $CdCl_2$–$NiSO_4$–water system at different feed flowrates and feed concentration 5 ppm.

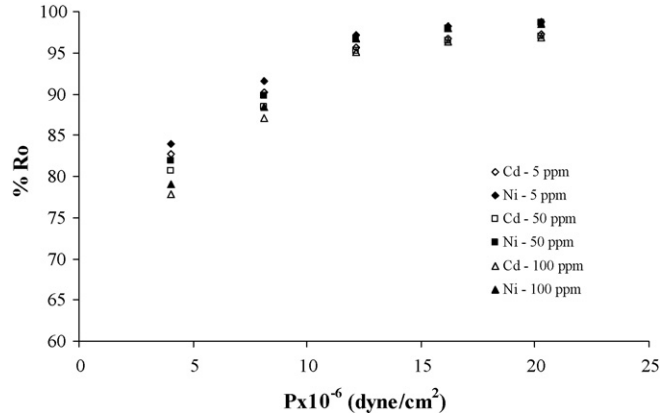

Fig. 7. Influence of applied pressure on the observed solute rejection of $CdSO_4$–$NiSO_4$–water system with different feed concentrations at feed flowrate of 15 L/min.

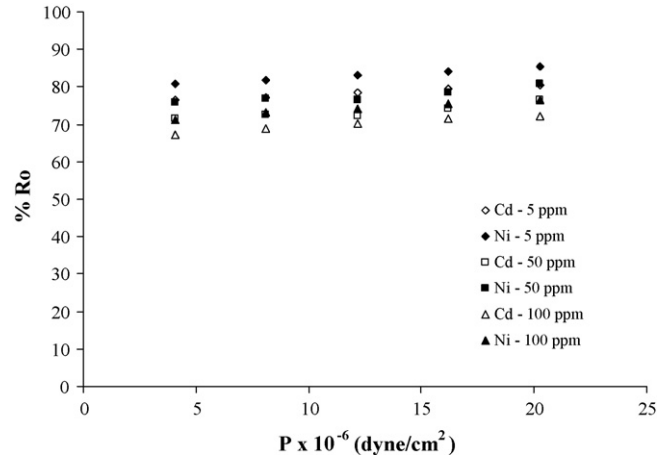

Fig. 8. Influence of applied pressure on the observed solute rejection of $CdCl_2$–$NiCl_2$–water system with different feed concentrations at feed flowrate of 5 L/min.

fixed at 5 ppm, 12 atm and 15 L/min, respectively. In the case of $CdSO_4$–$NiSO_4$–water system, there is no significant change in the rejection percentages of nickel and cadmium ions with pH change. Similar results were observed for nickel ion by Ahn et al. [10]. It can be seen from Fig. 9 that in the case of $CdCl_2$–$NiCl_2$–water system, the rejection is sensitive to pH change; R_O reached high at pH 1,

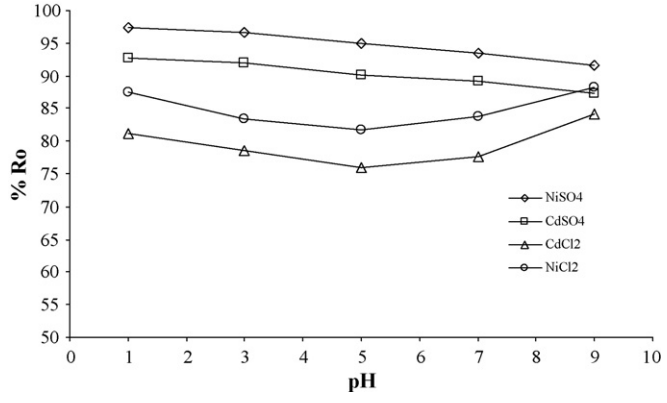

Fig. 9. Influence of pH on the observed solute rejection for $CdCl_2$–$NiCl_2$–water and $CdSO_4$–$NiSO_4$–water system (feed concentration = 5 ppm, applied pressure = 12 atm, and feed flowrate = 15 L/min).

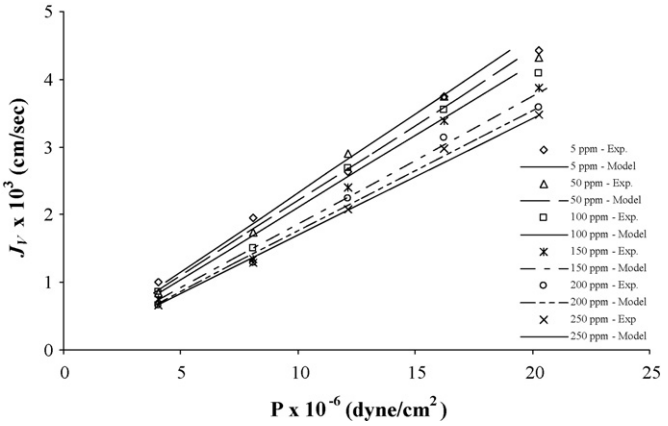

Fig. 10. Results from combined membrane transport and concentration polarization model for $CdCl_2$–$NiSO_4$–water system by using NF-300 membrane at different feed concentrations and a feed flowrate of 5 L/min.

then decreased to minimum at pH 5 and then increased at pH 7. In the present case, it may be said that at pH 5 the membrane isoelectric point (IEP) is approached. Similar IEP for cadmium ion was observed by Garba et al. [9] and Ballet et al. [17].

4.2. Determination of membrane transport parameters and boundary layer thickness

The non-linear parameter estimation program used to estimate the parameters, namely; hydraulic permeability (L_p), reflection coefficient (σ) and D_{AB}/δ; is based on the Levenberg–Marquardt method [31]. The permeate flux is taken at different operating pressures keeping feed flowrate and feed solute concentration constant for each set of data. The parameters L_p, σ, and D_{AB}/δ are estimated from Eq. (9). Theses parameters are then used to calculate applied pressure for different values of permeate flux (J_V). It can be seen from Fig. 10 that the model predictions for the pressure values are in good agreement with experimental results. The difference between experimental and model results increases when the pressure increases at lower concentration. It can be concluded that the model is still longer valid for a wide range of concentration (from 5 to 250 ppm) for binary salts.

The concentration of the solute at the surface of membrane (C_{A2}) is calculated using the film theory model given by Eq.

Table 1
Summary of the calculated values of L_P and D_{AB}/δ at various operating conditions for the binary salt system (PWP = 3.64×10^{-9} $cm^3/s\,dyn$).

Set	Feed rate (L/min)	Feed concentration (ppm)	$L_{P,\,Caculated}$ ($cm^3/s\,dyn$) $\times 10^9$	D_{AB}/δ (cm/s) $\times 10^3$
1	5	5	2.33	8.70
2	10	5	2.78	8.89
3	15	5	3.13	9.09
4	5	50	2.22	8.51
5	10	50	2.71	8.73
6	15	50	2.95	8.89
7	5	100	2.13	8.34
8	10	100	2.50	8.52
9	15	100	2.78	8.74
10	5	150	1.89	8.17
11	10	150	2.27	8.34
12	15	150	2.63	8.53
13	5	200	1.79	8.01
14	10	200	2.13	8.16
15	15	200	2.50	8.35
16	5	250	1.72	7.85
17	10	250	2.04	7.99
18	15	250	2.27	8.15

Table 2
Summary of the membrane transport parameters at various operating conditions for binary salt system.

Set	Feed rate (L/min)	Feed concentration (ppm)	Solute permeability $P_M \times 10^4$ (cm/s)		Reflection coefficient, σ	
			Cadmium	Nickel	Cadmium	Nickel
1	5	5	5.60	1.30	0.8920	0.9998
2	10	5	5.90	1.00	0.8864	0.9979
3	15	5	5.70	0.80	0.8749	0.9961
4	5	50	6.60	1.20	0.8641	0.9942
5	10	50	7.10	1.00	0.8548	0.9924
6	15	50	7.20	0.70	0.8455	0.9905
7	5	100	6.20	1.10	0.8381	0.9886
8	10	100	7.40	1.00	0.8236	0.9868
9	15	100	7.70	0.60	0.8121	0.9864
10	5	150	8.00	1.00	0.8047	0.9857
11	10	150	8.90	0.80	0.7972	0.9853
12	15	150	8.70	0.70	0.7809	0.9849
13	5	200	9.40	1.00	0.7749	0.9842
14	10	200	8.80	0.90	0.7638	0.9838
15	15	200	8.90	0.60	0.7508	0.9834
16	5	250	9.00	1.00	0.7433	0.9827
17	10	250	9.60	0.90	0.7303	0.9823
18	15	250	9.00	0.50	0.7065	0.9819

(2). The estimated parameters for the binary salt system used ($CdCl_2$–$NiSO_4$–water) in the present work are shown in Table 1. It can be observed from Table 1 that with increase in feed flowrate, from 5 to 15 L/min, the value of D_{AB}/δ is increasing at same feed concentration; that means the concentration polarization boundary layer thickness directly affected by the flowrate in cross-flow mode. Thus, the straightforward way of minimizing concentration polarization, to some extent, is to reduce the boundary layer thickness by increasing shear force at the membrane surface with high feed flowrates [32]. Eq. (5) can be rearranged by putting the value of β, to get [13],

$$J_V = \frac{P_M}{1-\sigma} \ln\left[\frac{\sigma(1-R)}{(\sigma-R)}\right] \tag{10}$$

In case of binary salt ($CdCl_2$–$NiSO_4$–water) system, the P_M can be obtained from the slope of plot of J_V vs. the coefficient of P_M on the right-hand-side of Eq. (10); by non-linear curve fitting method. These plots are shown in Fig. 11 for the cadmium ions and in Fig. 12 for nickel ions at different feed concentrations (5–250 ppm) and a feed flowrate of 5 L/min. The membrane parameters estimated by this method are summarized in Table 2. It can be seen from Table 2 that the σ decreases with increase in feed solute concentration, while the P_M decreases with co-ion valency. Such trend was observed in the literature in the case of Spiegler–Kedem model for NF membranes for different salts of cadmium and copper [17,18]. Mehiguene et al. [18] investigated the effect of the nature of co-ion on the retention, and found that the σ for each salt increases with co-ion valency, while the P_M decreases with co-ion valency. Ballet et al. [17] found that the value of P_s is highly dependent on the type of anion of the electrolyte solute. Strongly solvated anions (SO_4^{2-}) lead to lower values of P_s in comparison with the less solvated anions (NO_3^-). The σ is higher for sulphate than monovalent anions. Similar trend was observed by Garba et al. [9] and Ahn et al. [10] in the case of cadmium and nickel salts, respectively. The plot of true solute rejection (R) vs. J_V is shown in Fig. 13. It can be seen from Fig. 13 that the R calculated at various operating conditions increases with increasing feed flowrate and collapse onto a single line when plotted against the J_V. This unique correlation between the R and the J_V follows from the equation of irreversible thermodynamics model as given by Eq. (10). These plots exhibit a generalized relationship in a sense that they incorporate the effect of operating pressure and feed flowrate. It can be observed from Fig. 13 that the R is higher for the sulphate ions as compared to the chloride ions, which can be explained by the fact that the size of the former ion is larger than the latter [33].

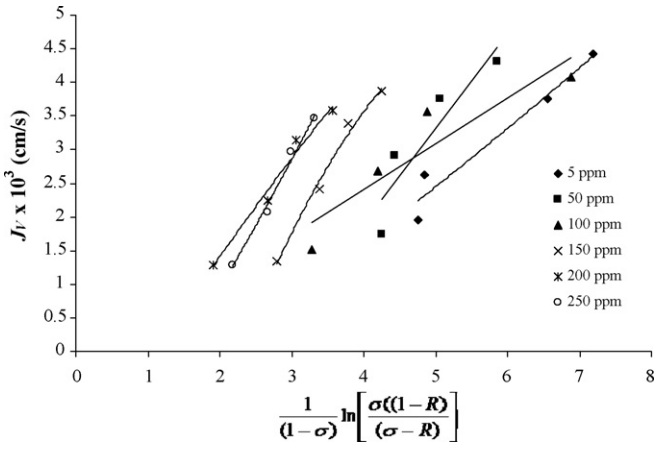

Fig. 11. Plot of permeate volume flux as a function of R for the cadmium ions to determine the overall solute permeability by non-linear curve fitting method at a feed flowrate of 5 L/min.

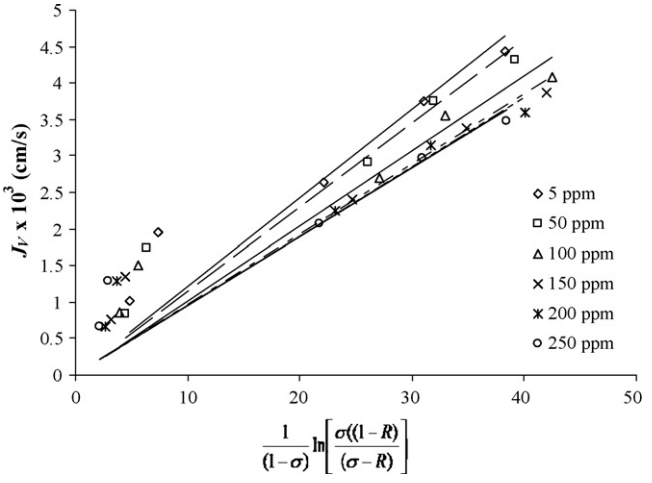

Fig. 12. Plot of permeate volume flux as a function of R for the nickel ions to determine the overall solute permeability by non-linear curve fitting method at a feed flowrate of 5 L/min.

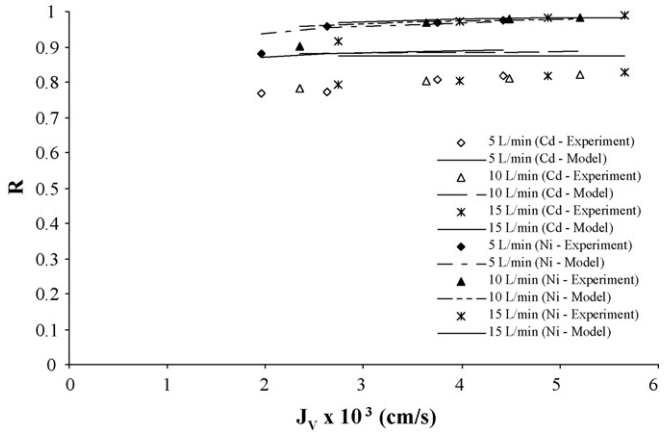

Fig. 13. Plot of true rejection (R) vs. permeate flux (J_V) and its comparison with the values calculated using irreversible thermodynamics model for the $CdCl_2$–$NiSO_4$–water system by using NF-300 membrane at different feed flowrate and feed concentration 5 ppm.

5. Conclusions

In the present study performance of a Perma-TFC-NF-300 membrane has been studied to separate heavy metals (nickel and cadmium) from aqueous binary metal solutions. The observed retention sequence is observed to be $R_O(Ni^{2+}) > R_O(Cd^{2+})$. Also, the NF-300 membrane is characterized by using the Spiegler–Kedem model coupled with the film theory of the concentration polarization. The estimated membrane transport parameters and the boundary layer thickness (in terms of D_{AB}/δ) are used to predict the performance of the membrane, in terms of ΔP and R, which showed about 10% deviation from the experimental results. The results show that σ and P_M depend on the type of anion of the particular salt, which is in line with the published literature. The model indicated that the true solute rejection of a membrane is a unique function of the permeate volume flux through the membrane for a binary salts under the operating conditions used in this study.

Acknowledgements

The first author (ZVPM) acknowledges the financial support from the Ministry of Human Resources Development, Government of India, New Delhi, India, under the TAPTEC Research Grant. Thanks are due to Mr. V.Y. Jose, Director, Permionics Limited, Vadodara, India, for providing the Perma-TFC-NF-300 membranes.

References

[1] T.A. Kurniawan, G.Y.S. Chan, W.-H. Lo, S. Babel, Physico-chemical treatment techniques for wastewater laden with heavy metals, Chem. Eng. J. 118 (2006) 83–98.
[2] N. Fiol, I. Villaescusa, M. Martinez, N. Miralles, J. Poch, J. Serarols, Sorption of Pb(II), Ni(II), Cu(II) and Cd(II) from aqueous solution by olive stone waste, Sep. Purif. Technol. 50 (2006) 132–140.
[3] S. Basha, Z.V.P. Murthy, B. Jha, Biosorption of hexavalent chromium by chemically modified seaweed, *Cystoseira indica*, Chem. Eng. J. 137 (2008) 480–488.
[4] N. Adhoum, L. Monser, N. Bellakhal, J.-E. Belgaied, Treatment of electroplating wastewater containing Cu^{2+}, Zn^{2+} and Cr(VI) by electrocoagulation, J. Hazard. Mater. 112 (2004) 207–213.
[5] J.U.K. Oubagaranadin, N. Sathyamurthy, Z.V.P. Murthy, Evaluation of Fuller's earth for the adsorption of mercury from aqueous solutions: a comparative study with activated carbon, J. Hazard. Mater. 142 (2007) 165–174.
[6] J.J. Qin, M.N. Wai, M.H. Oo, H. Lee, A pilot study for reclamation of a combined rinse from a nickel plating operation using a dual-membrane UF/RO process, Desalination 161 (2004) 155–167.
[7] N. Lamba, Z.V.P. Murthy, R. Kumar, Membrane processing of an aqueous waste stream from catalyst manufacturing plant, Sep. Sci. Technol. 37 (2002) 191–202.
[8] A.W. Mohammad, R. Othaman, N. Hilal, Potential use of nanofiltration membranes in treatment of industrial wastewater from Ni–P electroless plating, Desalination 168 (2004) 241–252.
[9] Y. Garba, S. Taha, N. Gondrexon, J. Cabon, G. Dorange, Mechanisms involved in cadmium salts transport through a nanofiltration membrane: characterization and distribution, J. Membr. Sci. 168 (2000) 135–141.
[10] K.H. Ahn, K.G. Song, H.Y. Cha, I.T. Yeom, Removal of ions in nickel electroplating rinse water using low-pressure nanofiltration, Desalination 122 (1999) 77–84.
[11] L.S. Clesceri, A.E. Greenberg, A.D. Eaton, Standard Methods for the Examination of Water and Wastewater, 20th ed., American Public Health Association, American Water Work Association, and Water Environment Federation, Washington, DC, 1998.
[12] A.E. Yaroshchuk, Rejection of single salts versus transmembrane volume flow in RO/NF: thermodynamic properties, model of constant coefficients, and its modification, J. Membr. Sci. 198 (2002) 285–297.
[13] V.K. Gupta, S.T. Hwang, W.B. Krantz, A.R. Greenberg, Characterization of nanofiltration and reverse osmosis membrane performance for aqueous salt solutions using irreversible thermodynamics, Desalination 208 (2007) 1–18.
[14] V. Gekas, B. Hallstrom, Mass-transfer in the membrane concentration polarization layer under turbulent cross flow. 1. Critical literature—review and application of existing Sherwood correlations to membrane operations, J. Membr. Sci. 30 (1987) 153–170.
[15] Z.V.P. Murthy, S.K. Gupta, Estimation of mass transfer coefficient using a combined nonlinear membrane transport and film theory model, Desalination 109 (1997) 39–49.
[16] O. Kedem, K. Spiegler, Thermodynamics of hyperfiltration (reverse osmosis): criteria for efficient membranes, Desalination 1 (1966) 311–326.
[17] G.T. Ballet, L. Gzara, A. Hafiane, M. Dhahbi, Transport coefficients and cadmium salt rejection in nanofiltration membrane, Desalination 167 (2004) 369–376.
[18] K. Mehiguene, Y. Garba, S. Taha, N. Gondrexon, G. Dorange, Influence of operating conditions on the retention of copper and cadmium in aqueous solutions by nanofiltration: experimental results and modeling, Sep. Purif. Technol. 15 (1999) 181–187.
[19] S. Koter, Determination of the parameters of the Spiegler–Kedem–Katchalsky model for nanofiltration of single electrolyte solutions, Desalination 198 (2006) 335–345.
[20] M. Soltanieh, W.N. Gill, Review of reverse osmosis membranes and transport models, Chem. Eng. Commun. 12 (1981) 279–363.
[21] A.L. Ahmad, M.F. Chong, S. Bhatia, Mathematical modeling of multiple solutes system for reverse osmosis process in palm oil mill effluent (POEM) treatment, Chem. Eng. J. 132 (2007) 183–193.
[22] Z.V.P. Murthy, S.K. Gupta, Sodium cyanide separation and parameters estimation for reverse osmosis thinfilm composite polyamide membrane, J. Membr. Sci. 154 (1999) 89–103.
[23] Z.V.P. Murthy, S.K. Gupta, Thinfilm composite polyamide membrane parameters estimation for the phenol–water system by reverse osmosis, Sep. Sci. Technol. 33 (1998) 2541–2557.
[24] C. Bhattacharjee, P.K. Bhattacharya, Ultrafiltration of black liquor using rotating disk membrane module, Sep. Purif. Technol. 49 (2006) 281–290.
[25] A. Apelblat, E. Korin, The vapour pressures over saturated aqueous solutions of cadmium chloride, cadmium bromide, cadmium iodide, cadmium nitrate, and cadmium sulphate, J. Chem. Thermodyn. 39 (2007) 1065–1070.
[26] M.E.L. Guendouzi, A. Mounir, A. Dinane, Water activity, osmotic and activity coefficients of aqueous solutions of Li_2SO_4, Na_2SO_4, K_2SO_4, $(NH_4)_2SO_4$, $MgSO_4$, $MnSO_4$, $NiSO_4$, $CuSO_4$, and $ZnSO_4$ at T = 298.15 K, J. Chem. Thermodyn. 35 (2003) 209–220.
[27] J.M.M. Peeters, J.P. Boom, M.H.V. Mulder, H. Strathmann, Retention measurements of nanofiltration membranes with electrolyte solutions, J. Membr. Sci. 145 (1998) 199–209.
[28] Y. Garba, S. Taha, J. Cabon, G. Dorange, Modeling of cadmium salts rejection through a nanofiltration membrane: relationships between solute concentration and transport parameters, J. Membr. Sci. 211 (2003) 51–58.
[29] N. Frares, S. Taha, D. Dorange, Influence of the operating conditions on the elimination of zinc ions by nanofiltration, Desalination 185 (2005) 245–253.
[30] P. Vanysek, Ionic conductivity and diffusion at infinite dilution, in: D.R. Lide (Ed.), CRC Handbook of Chemistry and Physics, 84th ed., CRC Press, Boca Raton, FL, 2005.
[31] M.S. Bazaraa, H.D. Sherali, C.M. Shetty, Nonlinear Programming Theory and Applications, 2nd ed., John Wiley & Sons, NJ, 1993.
[32] S.Y. Vaidya, A.V. Simaria, Z.V.P. Murthy, Reverse osmosis transport models evaluation: a new approach, Indian J. Chem. Technol. 8 (2001) 335–343.
[33] A.W. Mohammad, N. Hilal, H. Al-Zoubi, N.A. Darwish, Prediction of permeate fluxes and rejections of highly concentrated salts in nanofiltration membrane, J. Membr. Sci. 289 (2007) 40–50.